Analyst

Accepted Manuscript

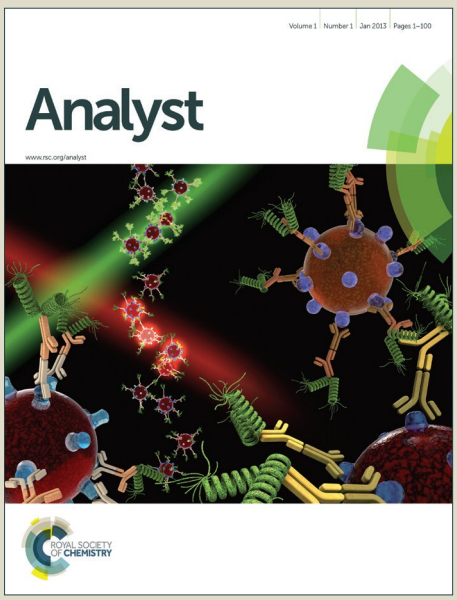

ROYAL SOCIETY OF CHEMISTRY

www.rsc.org/analyst

Analyst

ARTICLE

Remote Calorimetric Detection of Urea via Flow Injection Analysis

David E Gaddes[a], Melik Demirel[a,b], W. Brian Reeves[c], and Srinivas Tadigadapa[a,d]

Received 00th January 20xx,
Accepted 00th January 20xx

DOI: 10.1039/x0xx00000x

www.rsc.org/

The design and development of a calorimetric biosensing system enabling relatively high throughput sample analysis is reported. The calorimetric biosensor system consists of a thin (~20 µm) micromachined Y-cut quartz crystal resonator (QCR) as a temperature sensor placed in close proximity to a fluidic chamber packed with immobilized enzyme. Layer by layer enzyme immobilization of urease is demonstrated and its activity as a function of the number of layers, pH, and time has been evaluated. This configuration enables a sensing system where the transducer element is physically separated from the analyte solution of interest and thereby free from fouling effects typically associated with biochemical reactions occuring on the sensor surface. The performance of this biosensing system is demonstrated by detection of 1-200 mM urea in phosphate buffer via a flow injection analysis (FIA) technique. Miniaturized fluidics were used to provide continuous flow through a reaction column. Under this configuration the biosensor has an ultimate resolution of less than 1 mM urea and showed a linear response between 0 - 50 mM. This work demonstrates a sensing modality in which the sensor itself is not fouled or contaminated by the solution of interest and the enzyme immobilized Kapton® fluidic reaction column can be used as a disposable cartridge. Such a system enables reuse and reliability for long term sampling measurements. Based on this concept a biosensing system is envisioned which can perform rapid measurements to detect biomarkers such as glucose, creatinine, cholesterol, urea and lactate in urine and blood continuously over extended periods of time.

Introduction

Concentration of urea in blood and urine samples is an indicator of liver and kidney function and accordingly many biosensors have been proposed to quantify the concentration of urea. Electrochemical urea biosensors including amperometric [1, 2], potentiometric [3, 4], and field effect [5] sensors have been the extensively investigated and reported due to their simplicity. Colorimetric methods have been also been explored as a simple and inexpensive alternative [6]. Despite successful demonstration of these techniques, difficulties due to fouling of the sensor in the case of electrochemical sensors, limited dynamic range in the case of colorimetric sensors, and bias from endogenous molecules arising from pH variations or changes in the optical properties of the solution have prevented their widespread adaptation. Calorimetric sensors, detect the heat of reaction and, are directly biased by molecules of interest especially when catalyzed by bioselective molecules such as enzymes and are easily integrated into a continuous monitoring configuration and offer a general detection principle that is the focus of the work presented here.

A major advantage to the calorimetric sensing mechanisms is its universality since most biological processes are either exothermic or endothermic in nature [7] and thus provide a broad based platform for the sensing of biochemical reactions. Development of micromachined thermal sensors allow for the construction of small sized and adequately fast response time for the quantification of biochemical reactions and thus realize biosensors [8]. Enzyme thermistors employing a fluidic channel containing immobilized enzymes and miniaturized thermistors were one of the first miniaturized calorimetric sensors [9]. Since then calorimetric sensing of a wide range of analytes such as lactose, sucrose, glucose, galactose, urea, creatinine etc. have been demonstrated [10-12]. Zhang et al. demonstrated an integrated microcalorimeter with microfluidic channels and thin film thermopile arrays and successfully demonstrated enzymatic detection of glucose, urea, and hydrogen peroxide [13]. Commercial chip calorimeters, most notability from Xensor, have been extensively used to determine properties of various enzymes and liquids [14]. Further these nanocalorimeters have been used to monitoring metabolic heat production by biofilms [15], bacteria and fish embyros, displaying excellent sensitivities with signal noises less than 10 nW [16]. The highest sensitivity nanocalorimeter was able to resolve 4.2 nW in 3.5 nL of sample [17]. Although micromachined nanocalorimeters exhibit excellent thermal characteristics, immobilization of enzymes and the direct integration of microfluidics on these devices has proved to be difficult. While reduction of sample

[a] Department of Biomedical Engineering, The Pennsylvania State University, University Park, PA, USA.
[b] Department of Engineering Science and Mechanics, The Pennsylvania State University, University Park, PA, USA.
[c] Department of Nephrology, Milton S. Hershey College of Medicine, The Pennsylvania State University, University Park, PA, USA
[d] Department of Electrical Engineering, The Pennsylvania State University, University Park, PA, USA. E-mail: sat10@psu.edu, Tel. +1 814 865 2730.
† Footnotes relating to the title and/or authors should appear here.
Electronic Supplementary Information (ESI) available: [details of any supplementary information available should be included here]. See DOI: 10.1039/x0xx00000x

volume to microliters of volume may be beneficial in cases where sample is expensive, further reduction to nanoliters of samples is not necessarily desirable since the total signal output, for a given concentration, decreases in proportion to the volume of the sample and the reduced reproducibility, due to inhomogeneities in samples, decreases the overall confidence in the measurements. Furthermore, direct integration of the enzyme layer on the sensor surface leads to fouling of the sensors and the eventual degradation of the immobilized enzymes which are irreversibly intertwined with the sensor performance limit the device reproducibility and longevity [18]. Additional protection to prevent fouling and system instability have been found to be at the expense of the overall sensitivity performance [19]. Finally, microcalorimeter chips and their associated microfluidics and transduction electronics are not as inexpensive as the screen printed disposable electrodes, therefore, reuse of the sensor would be beneficial. Here we present a biosensing system utilizing a highly sensitive Y-cut quartz resonator as a temperature/infrared sensor enabling the physical separation of the analyte fluidics and the associated biochemistry from the thermal sensor chip and electronics, thus yielding a sensitive and robust biosensing system and capable of continuous flow injection analysis of urea.

Thermally sensitive shear mode (Y-cut) quartz resonators are used as the temperature detection elements in this work due to their extraordinary temperature resolutions of 10^{-6} °C and exceptional signal to noise ratio (SNR)temperature sensitivity performance [20, 21]. Quartz resonator based temperature sensors exhibit 2 – 3 orders of magnitude higher temperature SNR performance when compared to other temperature sensors such as thermopiles and thermistors. Our group has previously demonstrated a proof-of-concept biosensor based on this principle capable of batch testing urea and glucose [22]. However, the demonstrated proof-of-concept sensor used droplets of enzymes that limited the sensor to batch testing only and was not capable of high throughput and repeated measurements. This paper clearly advances from our previous work on remote calorimetry though the use of packed column of layer-by-layer immobilized urease on glass beads and integration of fluidic system for flow injection analysis for rapid and high throughput detection and a novel disposable enzyme cartridge concept that allows for repeated use of the micromachined thermal sensor and its associated electronics to achieve injection flow analysis system. Through these improvements, we have been able to achieve ~20 times improvement in the sensitivity of urea in comparison to our previous work.

The biosensing system presented here is schematically illustrated in Fig. 1(a). The temperature sensitive Y-cut quartz resonator is placed in close proximity to a thin fluidic column in which thermal energy is produced, in this case, by the hydrolysis of urea catalyzed by immobilized urease. Figure 1(b) shows the cross-sectional view of the sensing system. It consists of the reaction column traversing across a 100 µm thick stainless steel plate to which the sensor is attached on the back side as shown. Glass beads containing immobilized enzyme are packed into the Kapton® tubing and held in place using a frit, while the analyte is passed through the reaction column. As the enzyme mediated analyte reaction occurs in this region, heat produced is transferred to the sensor via the through hole in the stainless steel plate. Heat transfer between the reaction flow tube to the sensor occurs through the enclosed column of air by conduction as well as through direct radiative coupling. In this manner the concentration of urea in a solution may be determined by thermally induced frequency shift of the sensor.

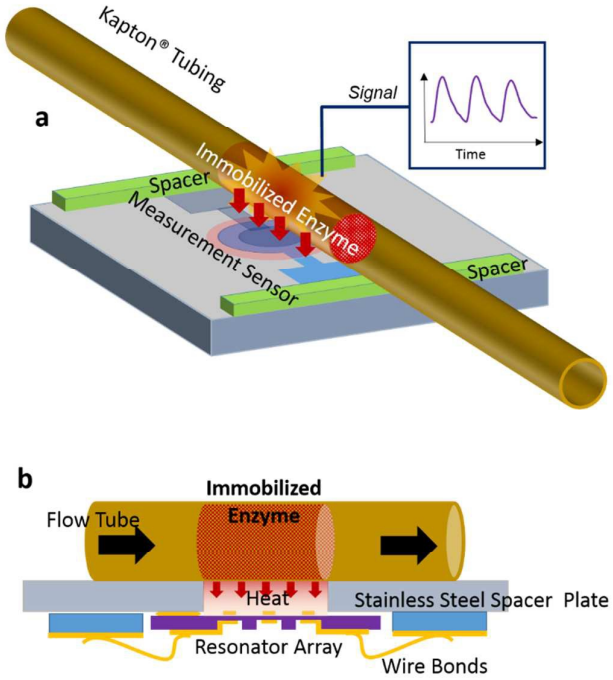

Fig. 1 (a) Oblique 3D schematic of the complete sensing system. The reaction column resides on top of a 100 µm stainless steel plate (spacer). Enzyme functionalized glass beads are packed into the Kapton® tubing and held in place by a frit. The close proximity of the Kapton® tubing reaction chamber to the quartz resonator temperature sensor results in a very sensitive non-contact coupling of the heat of the reaction through conduction by air and radiation. (b) A cross-sectional illustration of the sensor system. The enzyme functionalized section of the Kapton® tubing spans the through-hole in the stainless steel plate across which the sensor resonator is located.

Experimental section

Sensor Design and Function

The biosensing system presented here utilizes a Y-cut quartz based temperature/thermal infrared sensor fabricated in house. A 100 µm thick wafer Y-cut quartz 1" in diameter was micromachined to produce arrays of high frequency, 62 MHz, resonators operating in thickness shear mode. The fabrication process of these highly sensitivity devices is reported by our group elsewhere [20]. The sensor array was packaged on a stainless steel plate 100 µm in thickness using an electrically conductive epoxy and wire bonded onto bond pads attached to the stainless steel plate as shown in Fig. 1(b) and Fig. 2(a). These bond leads are electrically connected to gold SubMiniature version A (SMA) coaxial RF connectors displayed on the side of the sensor package. A stainless steel manifold was fabricated to hold the reaction column in place which is

mounted onto the steel plate holding our device as shown in the Fig. 2(b). The series resonance frequency of the Y-cut quartz resonator was monitored using an Agilent 4395A impedance analyzer. The typical admittance characteristics of the resonator is shown in Fig. 3. The biochemical reaction is monitored by tracking a fixed

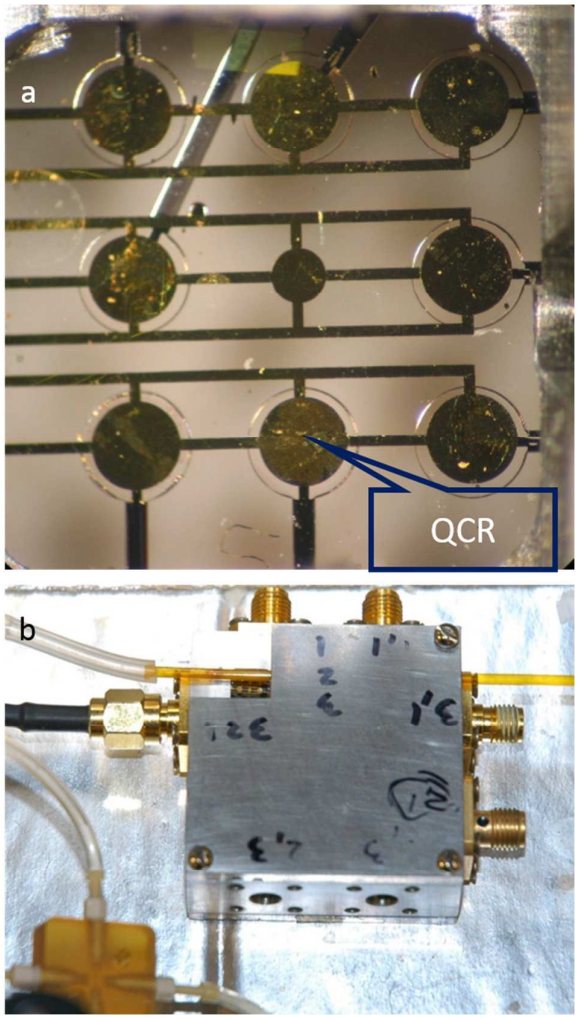

Fig. 2 (a) Optical picture of the quartz resonator array attached to the stainless steel plate with conductive epoxy and wire bonded to the gold pads for connection to the SMA connector. Arrows point to two of the eight resonators (b) Packaged device with the stainless steel manifold showing the aligned placement of the Kapton® tubing with the resonator array. The resonator is below the stainless-steel plate whereas the Kapton® tubing spans in tight contact to the stainless-steel plate ensuring a gap of 100 µm.

frequency point between the two inflection points, the *linear region (a-b),* of the susceptance (imaginary component of admittance) over time as indicated also in Fig. 3. The Agilent impedance analyzer is capable of tracking 801 points over a single scan. This method of monitoring the admittance provides superior time resolution as compared to scanning a set of frequency points to obtain a full scans of the admittance.

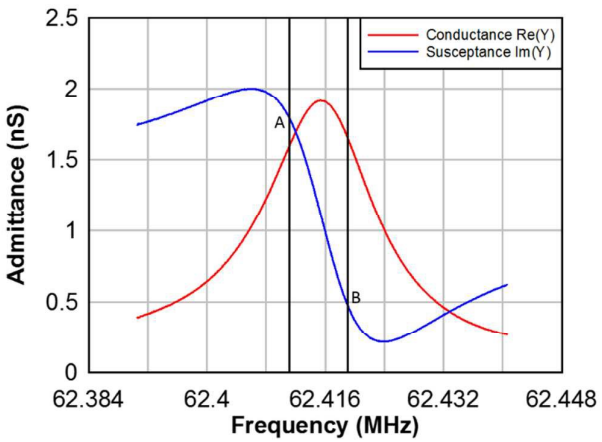

Fig. 3 The experimentally obtained admittance characteristic of the resonator with the linear region of susceptance indicated between the points A-B.

Miniaturized Fluidic Set-up

Miniaturized valves and pumps purchased from Labsmith® (Livermore, CA) were used to provide continuous flow through the reaction column packed with urease immobilized glass beads. Analyte of different molarities was prepared in 0.1 M phosphate buffer, pH 6.8. These pumps were programmed to provide 100 µl of analyte followed immediately by 200 µl 0.1 M phosphate buffer pH 6.8; all pumped at 100 µl/min. These steps were repeated in order to provide continuous flow for the duration of the experiment. Figure 4(a) shows the pumping scheme used in this work schematically and Fig. 4 (b) shows an optical image of the fluidic set-up.

Layer by Layer (LBL) Immobilization and Fabrication of Reaction Column

Urease was immobilized on soda lime glass beads 30 – 50 µm in diameter (Polysciences Inc. Warrington, PA) using two polyelectrolytes: branched polyethylenimine molecular weight 200 kids and polystyrene suflonate molecular weight 70 kDa (Sigma-Aldrich Saint Louis, MI). Prior to use 300 mg of the glass beads were subjected to a piranha clean (5:3::H_2SO_4:H_2O_2). These beads were then thoroughly washed with deionized water and collected using a Büchner funnel with 10 – 20 µm pores (Sigma-Aldrich Saint Louis, MO) and a vacuum filtration flask (Sigma-Aldrich Saint Louis, MO). Prior to enzyme immobilization, precursor polyelectrolyte layers were formed on the glass bead in the following manner. The beads were transferred to a vial containing 10 ml of 5 µM branched polyethylenimine (BPEI) pH 8.6 in aqueous solution and stirred at 800 rpm for 10 minutes with a magnetic stir bar. Next the BPEI solution containing beads was filtered using the Büchner funnel and vacuum filtration flask. The beads were washed with DI water for 2 minutes and again filtered. Following absorption of BPEI the beads were placed in a vial with 10 ml

aqueous

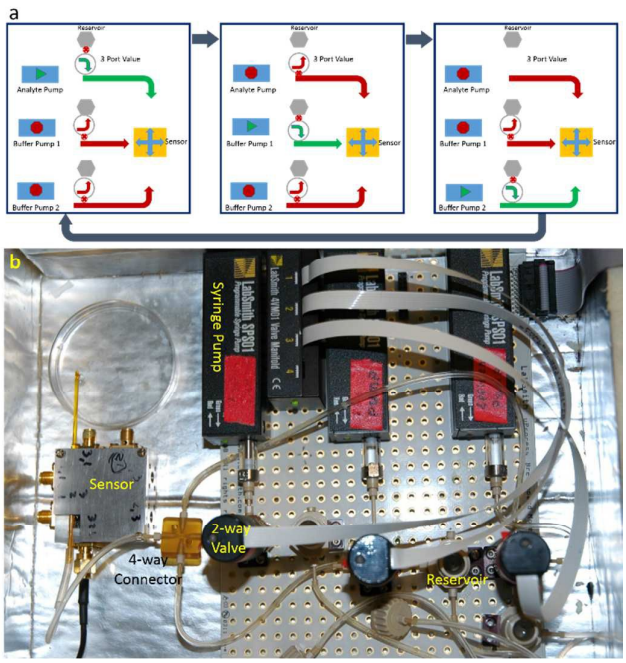

Fig. 4 (a) Schematic illustration of the pumping scheme employed during testing of the sensor. (b) Optical photograph of the fluidic system.

solution of 5 µM polystyrene sulfonate (PSS) pH 6.6. Again the solution was stirred at 800 rpm for ten minutes before filtration and subsequent washing. These two polyelectrolyte deposition steps were repeated to obtain two alternating layers each of BPEI and PSS and was followed by another layer of BPEI absorption to obtain glass-(BPEI-PSS)$_2$-BPEI. Next, urease was immobilized onto this silica bead. This was accomplished by creating a 10 ml solution of 1 mg/ml urease in a 50 mM phosphate buffer solution at pH 8.15. The beads were placed in a vial with the enzyme solution and were stirred for 10 minutes before washing with 50 mM phosphate buffer for 2 minutes. The BPEI and enzyme steps were alternatively repeated to create the desired number of layers of enzyme on the bead to result in glass-(BPEI-PSS)$_2$-(BPEI-Enzyme)$_n$.

The fluidic reaction column was made by packing the above functionalized glass beads containing immobilized urease in a Kapton® tubing (Amazon LLC) with wall thickness .00125" (31.75 µm) and ID 0.0666" (1.692 mm) creating a packed column ½" long. A frit was placed in the tubing to hold the LBL immobilized beads in place on one end.

Evaluation of immobilized urease catalytic activity

The activity of immobilized urease was characterized by a colorimetric assay using a fluorescent pH sensitive dye hydroxypyrene-3,6,8-trisulfonic (Sigma-Aldrich Saint Louis, MI). A solution of 0.1 M phosphate buffer was adjusted to pH 6.2, the start on the linear region (pH 6.2-8). This buffered solution was used to create a solution of 20 mM Urea (Sigma-Aldrich Saint Louis, MI) and 2 mM 1-hydroxypyrene-3,6,8-trisulfonic (HTPS). A 500 µm thick piece of borofloat glass was immobilized with 0, 1, 3, 5, and 7 layers of urease using the procedure described above. These glass pieces were placed into a 96 well plate. To the well plate 110 µl of the solution containing urea and HTPS was added. The solution was monitored at 10 second intervals for 20 minutes using a Tecan F200 PRO plate reader. The excitation and emission filters on the plate reader were set to wavelengths of 460 nm and 510 nm respectively. To correct for fluorescent quenching the signal obtained from the well with glass piece containing 0 layers of urease was collected.

Decay of layer-by-layer immobilization

The decay of the biosensing system due to the loss of the layer-by-layer immobilized enzyme and denaturation over time was investigated at room temperature. Determination of this decay was conducted by using the same reaction column over a two week period. The reaction column placed into the sensing package with 50 mM solution reacting in the same manner described in section 2.2. The reaction column was stored in 0.1 M phosphate buffer at pH 6.8 in between measurements. To obtain accurate results the reaction column was not removed from the sensor package in the two week period.

Sensor Response to pH

The dependence between the output of our calorimetric biosensing system and pH of the urea containing solution was studied. The pH of the solutions containing 50 mM urea in 0.1 M phosphate buffer and the 0.1M phosphate buffer subsequently used to wash the reaction chamber were adjusted to the following pH values: 5.8, 6.3, 6.8, 7.5, and 8.2. Prior to testing at a particular pH the reaction column was washed using a buffer solution with the same pH. Following each experiment the biosensing system was tested using a solution of pH 6.7 to ensure no degradation to the system occurred.

Results and discussion

Device Properties, Characteristics and Measurement Technique

The series resonance of the resonator used in this paper at room temperature was measured to be 62.416 MHz. The temperature sensitivity of the Y-cut quartz resonator was determined by placing the resonator in an oven and varying the temperature from 23-28 °C. A linear relationship between temperature and resonance frequency was observed and the temperature sensitivity was determined to be 5.42 kHz/°C implying a temperature sensitivity of 87 ppm/°C which is very close of the expected value of 90 ppm/°C temperature sensitivity of Y-cut quartz. Using the measurement method of tracking susceptance at a fixed frequency described in section 2.4 the Allan deviation of this resonator was calculated to be 3.76 Hz using a time constant of 2.24 seconds. Based upon the experimentally obtained temperature sensitivity for the 62 MHz device, the Allan deviation is equivalent to a temperature

fluctuation of 0.694 m°C and therefore should be able to resolve temperature signals of ~1 millidegrees.

Simulations were performed to determine how the spacing between the reaction tube and the sensor affects the sensitivity. Using COMSOL® simulation software, the device configuration was set-up, meshed, and simulated using the heat transfer module. Results obtained showed that the primary heat transfer mechanism between the reaction tube and the sensor was through conduction through the trapped air between the two. A linear relationship between the gap and sensitivity was obtained with smaller gaps achieving higher sensitivity. The gap in our set-up is determined by the 100 μm thickness of the steel plate that was used for packaging the device and could not be reduced by much more since steel plates of smaller thickness were mechanically unstable and resulted in substantial stress in the quartz resonators resulting in unstable performance. The role of ambient temperature fluctuations was also examined. In the laboratory settings, we found that the ambient temperature fluctuations are fairly slow and increase and decrease monotonically. In relation to this, the signals obtained from the enzymatic reactions are much faster and thus the change in temperature signals can be readily seen. A differential measurement set-up is expected to improve the signal to noise ratio, however, this will be implemented in future work. Furthermore, we also examined the dependence of the rate of the enzymatic reaction as a function of temperature between 20 ♯C and 37 ♯C and found that for urease catalysed hydrolysis of urea, the reaction rate was not significantly affected by changes in temperature. Since ambient temperature fluctuations are only in the range of a couple of degrees, the errors are expected to be minimal. No additional quantification of errors due to ambient temperature fluctuations have not been considered.

Characterization and Optimization of Layer-by-Layer (LBL) Immobilization

Prior to implementing the LBL immobilization methodology in our biosensing system, the LBL immobilization of urease was characterized by analyzing the rate of urea hydrolysis through a colorimetric reaction over 30 minutes. A pH sensitive dye hydroxypyrene-3,6,8-trisulfonic (HTPS) was used to indicate the change in pH of the urea containing solution. The production of ammonia due to the catalytic hydrolysis of urea by urease results in an overall increase in the fluorescence of the HTPS molecules.

$$CO(NH_2)_2 + H_2O \xrightarrow{Urease} 2NH_3 + CO_2 \qquad (1)$$

A calibration experiment to determine the response from the plate reader against the pH of the solution was first conducted to determine the linear range of fluorescence change against pH of the HTPS dye and the slope of this linear range. Various layers of urease were immobilized to understand how the number of layers of enzyme will impact the rate of hydrolysis of urea, the results are displayed in Fig. 5. The rate of reaction due to 1 layer of immobilized enzyme is observed to be relatively slow, Fig 5(a). Three layers catalyzes at a sustainably higher rate while 5 layers again increases the rate of hydrolysis. The trend appears to stop at 7 layers where diffusion limitation or instability of the LBL structure seems to prevent any further increase in the rate of reaction. The reaction rate of each LBL sample was determined by the slope of the data collected by the plate reader and is shown in Fig. 5(b). This data suggests that 5 layers of urease are sufficient to maximize the detectivity of our sensing system.

Detection of exothermic urea hydrolysis by Y-cut quartz based infrared sensor array

Prior to any testing of our system an optimal flow rate was determined by using a reaction chamber packed with glass beads hosting 5 layers of enzyme. Experiments were conducted at 50, 75, 100, 125 and 150 μl/min. In all cases 100 μl of 50 mM urea containing solution was injected into the reaction chamber at each flow rate followed by 200 μl phosphate buffer. This process of analyte followed by the buffer was performed 4 times consecutively. The sensor output remains constant at lower flow rates up to 100 μl/min whereas at higher flow rates of 125 and 150 μl/min the amplitude of the sensors output is reduced due to the reduced residence time in the reaction zone at higher flow rates. Based on these results, the fastest flow rate 100 μl/min was chosen to minimize the test time.

The hydrolysis of urea produces 64 kJ/mol when catalyzed by urease and is enough heat to enable thermal detection. Beads

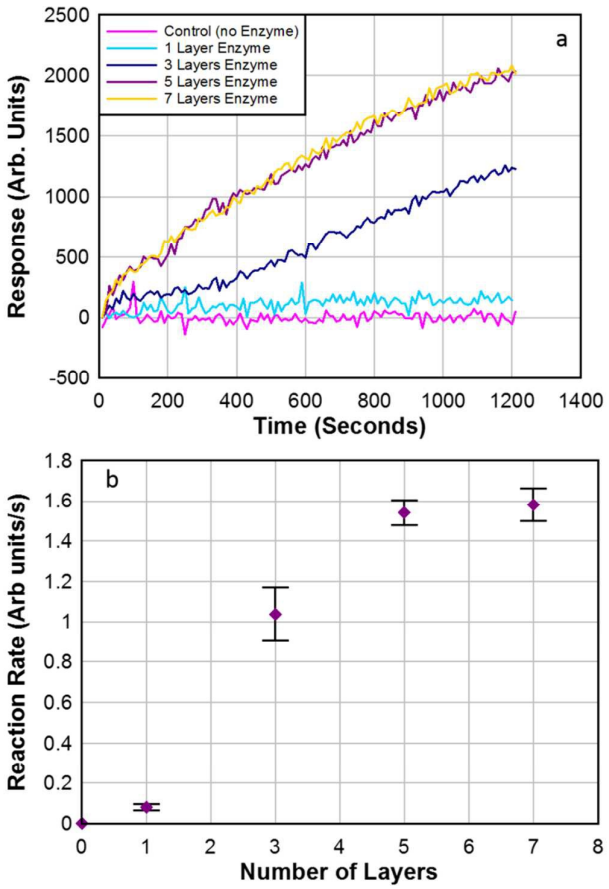

Fig. 5 Colorimetric Layer-by-layer Characterization. (a) Hydrolysis of urea by varying the number of layers of urease as monitored by pH sensitive dye. (b) Reaction rate as a function of the number of layers as determined from the initial linear region of the reaction. Standard deviation is determined from variations over 3 consecutive measurements.

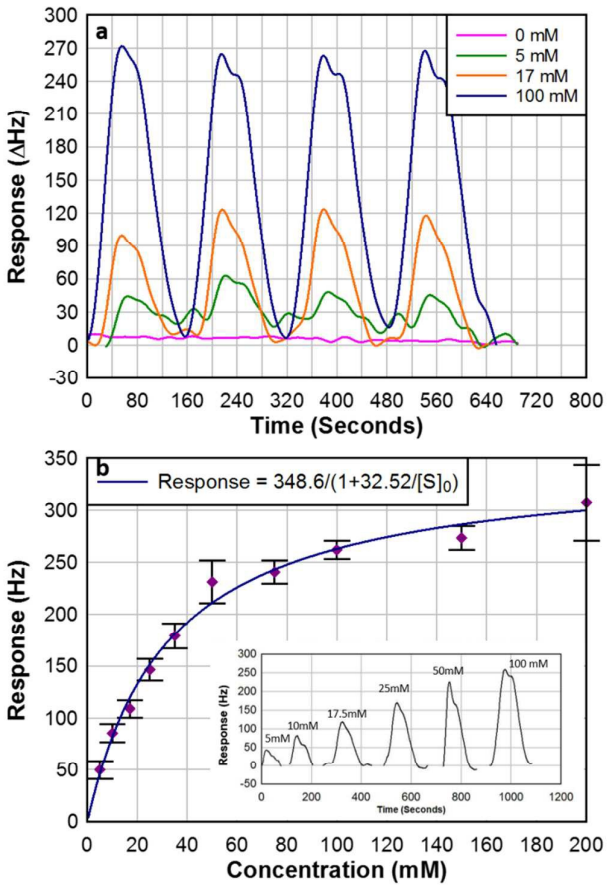

Fig. 6 Y-cut quartz resonator based detection of hydrolysis of urea catalyzed by urease. (a) Real-time sensor signal as a function of time as the analyte passes through the immobilized enzyme located above the resonator for some of the tested concentrations. (b) Peak height of the response plotted against concentration of urea. Standard deviation is obtained from the variations in response of 4 consecutive measurements. Inset shows the real-time signal for the various concentrations of urease.

packed into the Kapton® tubing containing 5 Layers of enzyme were used to catalyze the hydrolysis just above the resonator. For determining the sensitivity performance for urea detection,100 µl of a particular concentration was injected followed by 200 µl phosphate buffer and the process was consecutively repeated 4 times. The real-time response of the Y-cut quartz sensor to the flowing analyte of various concentrations is shown in Fig. 6(a). The peak height of the responses as shown in Fig. 6(b)inset are plotted against concentration in Fig. 6(b). Due to the outstanding sensitivity of the quartz thermal sensor, the non-contact biosensing system described here is able to resolve urea concentrations to below 1 mM.

A typical enzymatic reaction can be written as, E+S ☞ ES ❄ P, where E represents the enzyme, S the substrate, and P is the product. The rate of the reaction, v, can then be written as $v = k_b[ES]$ where [ES] represents the concentration of the enzyme-substrate complex formed and k_b is the rate constant for the formation of the product from the enzyme-substrate complex. The plot in Fig. 6(b) exhibits the typical Michaelis-Menton type

kinetics where the response (in Hertz) is proportional to product formation can be given by

$$v = \frac{k_b[E]_0}{1 + \frac{K_M}{[S]_0}} \qquad (2)$$

where $[E]_0$ is the total concentration of the immobilized enzyme in the flow tube, $[S]_0$ is the initial concentration of the substrate, and K_M is the Michaelis constant. Due to continuous flow of the analyte (i.e. continuous replenishment), the concentration of the analyte can be considered to be fixed at $[S]_0$, and thus the response of the sensor is representative of the initial velocity of the reaction for that concentration. Therefore, the Michaels-Menton kinetics analysis is valid for the data plotted in Fig. 6(b). Fitting the Michaelis-Menton equation to the experimental data gives a Michaelis constant K_M of 32.52 mmol/l for the immobilized urease on beads. This excellent reaction rate may be due to the large amount of enzyme immobilized on the beads as well as efficient mixing caused when the fluid passes through the packed column. Furthermore, the value of K_M obtained is similar to urease activities determined in studies on pig and cattle manure [23]. The complete reaction of 100 µl of 5 mM urea would produce 32 mJ of heat. From Fig. 6, the frequency signal obtained for 5 mM urea corresponds to ~39 Hz implying a temperature increase of the resonator of ~ 7 m°C. Based on the noise of the system, which has been measured to be better than 1 m°C, urea resolution of better than 1 mM can be obtained using the current sensor. Application of 32 mJ using a chromium wire heater in the flow tube resulted in a temperature change of 9 m°C in the resonator indicating a nearly complete, ~80%, reaction of the urea. Considering that the sensor has a resolution 0.7 m°C, the sensor is capable of measuring urea concentrations of less than 1 mM which is sufficient resolution for the biologically relevant urea levels for human urine which ranges from 100 mM – 300 mM or blood urea nitrogen levels which ranges from 2.5 mM – 7 mM.

Enzyme Decay over time

The longevity of the device is an important aspect of biosensors. Particularly, enzyme denaturation as well as loss of immobilized enzyme from the layer by layer structure will affect the effective lifetime of this biosensing system. Degradation of the sensing system was investigated by observing the response from the sensor to a 50 mM urea solution over a period of two weeks with the immobilized enzyme stored at room temperature during the entire period of the test. Data collected in this two week period is displayed in Fig. 7. Our system shows little decay for the first four days followed by an exponential decay with an e^{-1} decay time of additional ~4 days. This decay is likely due to the instability of the immobilization technique rather than enzyme degradation. Thus, a given immobilized enzyme loaded Kapton tube can be used continuously for several days. The sensing system is designed for the tubing to be easily replaced and although a calibration protocol is not shown here, it can be done using two standard solutions in the linear response region of the sensor for repeated use. The separation of the sensor/transducer element from the fluidic chamber and immobilized enzyme resulting in the non-contact mode of operation provides a convenient approach towards a robust and reproducible sensing system where the progressively decaying enzymatic module may easily be swapped.

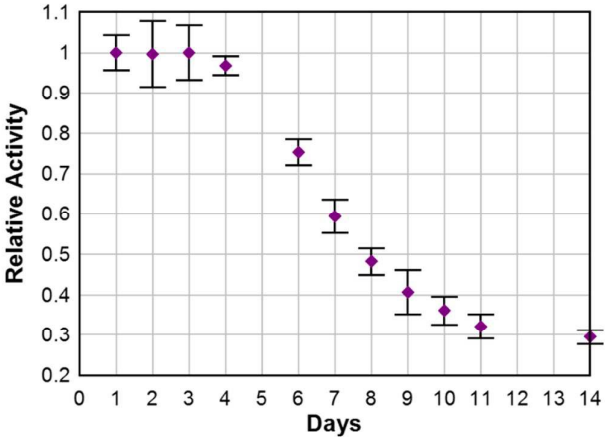

Fig. 7 Longevity of the immobilized urease on glass beads. Peak height of Y-cut quartz output in response to 50 mM urea over a period of 2 weeks. Standard deviation are obtained from the variations in response of 3 consecutive measurements.

Influence of solution pH on biosensor response and quality.

Due to the well-known effects of pH regarding enzymatic activity as well as the stability of the layer by layer immobilization, the biosensor was used to evaluate the variations in the response to urea solutions of varying pH. The biosensing system was assembled as described previously, however, the urea containing solution and wash buffer solutions were adjusted to the following values of pH: 5.8, 6.3, 6.8, 7.5, and 8.2. All experiments were done using 50 mM urea concentration. Prior to any test the reaction column was thoroughly washed with the appropriate pH buffer. The response of the sensor is shown in Fig. 8. The response of the biosensor reaches a maximum value for a pH of 6.8, and is close to the reported optimum pH for urease enzymatic activity [24]. Variation of pH in either direction leads to a decrease in sensor response. However, the decay is faster for lower values of pH. As a control, after each pH experiment the biosensor was checked for its stability using the urea solution at a pH of 6.8

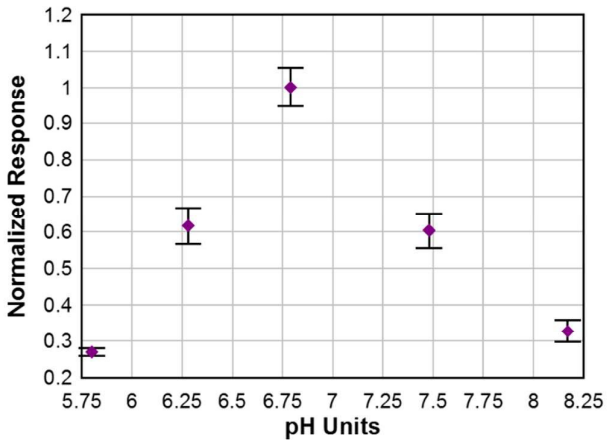

Fig. 8 Sensor response as a function of solution pH values of 5.8, 6.3, 6.8, 7.5, and 8.2 for 50 mM urea solution. Standard deviation is calculated from three consecutive measurements.

and to determine if the LBL immobilization was impacted upon exposure to the various pH solution. In all cases, except for the lowest pH, the LBL immobilization remained intact. Notably the isoelectric point of urease is 4.4, and thus a decrease of pH down to this level is expected to start to change the electrostatic charge on the enzyme and negatively impacts the LBL immobilization.

Conclusions

An efficient calorimetric sensing system based upon Kapton® flow tube filled with immobilized urease enzyme on glass beads is presented. Y-cut quartz resonator based thermal sensor was placed with a 100 μm of gap to the Kapton® flow reaction tube to detect the enzymatically catalysed heat of the reaction upon injection of urea containing solutions. A layer by layer enzyme immobilization technique on glass beads was explored for urease and was successfully used in the demonstration of the biosensing system. The sensing system showed a linear relationship between concentration and output for 1 – 50 mM urea concentrations. Based on the signal and noise measurements, the system is capable of resolving urea concentrations below 1 mM. The entire fluidic system has been automated through the use of miniaturized pumps and valves that can be controlled using a microcontroller to achieve repeated and near continuous measurement of the analyte solutions with specificity obtained through the use of the enzyme. The presented non-contact method of calorimetric sensing system is robust, reproducible, and is applicable to a wide variety of enzymatically catalysed biochemical reactions. The linear output range is in the clinically relevant regions for physiological glucose, creatinine and urea in biological solutions. The signal to noise ratio of the system could be further improved using a differential measurement system and is currently being investigated. The disposable nature of the immobilized enzyme fluidic reaction column, allows for easy to swap biosensor cartridge design for the sensor system to be used to quantify several metabolites of interest.

Acknowledgements

This work was supported in part by the Grace-Woodward Grant from Penn State University College of Engineering and College of Medicine. DG would like to thank Diefenderfer Fellowship from the College of Engineering, Penn State University.

Notes and references

1. M. Tyagi, M. Tomar and V. Gupta, Biosensors and Bioelectronics, 2013, 41, 110-115.
2. A. Jiménez, M. P. G. Armada, J. Losada, C. Villena, B. Alonso and C. M. Casado, *Sensors and Actuators B: Chemical*, 2014, **190**, 111-119.
3. B. Lakard, G. Herlem, S. Lakard, A. Antoniou and B. Fahys, *Biosensors and Bioelectronics*, 2004, **19**, 1641-1647.
4. S. V. Marchenko, I. S. Kucherenko, A. N. Hereshko, I. V. Panasiuk, O. O. Soldatkin, A. V. El'skaya and A. P. Soldatkin, *Sensors and Actuators B: Chemical*, 2015, **207**, 981-986.
5. Y.-H. Lin, S.-H. Wang, M.-H. Wu, T.-M. Pan, C.-S. Lai, J.-D. Luo and C.-C. Chiou, *Biosensors and Bioelectronics*, 2013, **43**, 328-335.
6. G. Gauglitz and M. Reichert, *Sensors and Actuators B: Chemical*, 1992, **6**, 83-86.
7. B. Danielsson, *Journal of Biotechnology*, 1990, **15**, 187-200.
8. A. W. van Herwaarden, *Thermochimica acta*, 2005, **432**, 192-201.
9. K. Mosbach and B. Danielsson, *Biochimica et Biophysica Acta (BBA)-Enzymology*, 1974, **364**, 140-145.
10. B. Danielsson, K. Gadd, B. Mattiasson and K. Mosbach, *Clinica Chimica Acta*, 1977, **81**, 163-175.
11. P. Bataillard, E. Steffgen, S. Haemmerli, A. Manz and H. M. Widmer, *Biosensors and Bioelectronics*, 1993, **8**, 89-98.
12. B. Mattiasson and B. Danielsson, *Carbohydrate research*, 1982, **102**, 273-282.
13. Y. Zhang and S. Tadigadapa, *Biosensors and Bioelectronics*, 2004, **19**, 1733-1743.
14. E. Iervolino, A. W. van Herwaarden and P. M. Sarro, *Thermochimica acta*, 2009, **492**, 95-100.
15. T. Hartmann, N. Barros, A. Wolf, C. Siewert, P. L. O. Volpe, J. Schemberg, A. Grodrian, E. Kessler, F. Hänschke, F. Mertens and J. Lerchner, *Sensors & Actuators: B. Chemical*, 2014, **201**, 460-468.
16. J. Lerchner, A. Wolf, H. J. Schneider, F. Mertens, E. Kessler, V. Baier, A. Funfak, M. Nietzsch and M. Krügel, *Thermochimica acta*, 2008, **477**, 48-53.
17. W. Lee, W. Fon, B. W. Axelrod and M. L. Roukes, *Proceedings of the National Academy of Sciences*, 2009, **106**, 15225-15230.
18. K. Ramanathan and B. Danielsson, *Biosensors and Bioelectronics*, 2001, **16**, 417-423.
19. R. J. Geise, J. M. Adams, N. J. Barone and A. M. Yacynych, *Biosensors and Bioelectronics*, 1991, **6**, 151-160.
20. P. Kao and S. Tadigadapa, *Sensors and Actuators A: Physical*, 2009, **149**, 189-192.

[21] M. B. Pisani, Ren, K., Kao, P., and Tadigadapa, S., *Journal of Microelectromechanical Systems*, 2011, **20**, 288 - 296.
[22] K. Ren, P. Kao, M. B. Pisani and S. Tadigadapa, *Analyst*, 2011, **136**, 2904-2911.
[23] X. Dai and H. Karring, *PLoS ONE*, 2014, **9**, e110402.
[24] B. H. van der Schoot and P. Bergveld, *Analytica Chimica Acta*, 1990, **233**, 49-57.